

Adaptive Interleaver Based on Rate-Compatible Punctured Convolutional Codes

Francesc Rey, Meritxell Lamarca, and Gregori Vazquez

Abstract—This letter focuses on the design of an adaptive Bit-Interleaved Coded Modulation (BICM) scheme for frequency selective slow fading channels where the transmitter has certain knowledge of the channel response. In particular, we consider the design of the interleaver stage for a specific convolutional code operating with OFDM modulation. The adaptive interleaver uses the puncturing tables of the Rate-Compatible Punctured Convolutional Codes (RCPC codes) to rearrange the bits as a function of the fading values and the specific constellation. The performance of different interleavers are compared, revealing that the adaptive RCPC-based interleaver produces larger Euclidean distances between the received codewords and reduces the packet error rate (PER), specially when the number of deep-faded subcarriers increases. Numerical results also evidence the importance of the interleaver choice when comparing the performance of different power allocation strategies.

Index Terms—Adaptive interleaver, bit-interleaved coded modulation (BICM), channel state information at the transmitter (CSIT), orthogonal frequency-division multiplexing (OFDM), rate-compatible punctured convolutional codes (RCPC).

I. INTRODUCTION

WHEN channel state information (CSI) is available at the transmitter it is possible to design the transmission stages to optimally adapt the transmitted signal to the channel conditions. This channel information has been generally used to design power and bit allocation strategies, as well as to adapt the coding rate (e.g. [1] and references therein). However, few works use CSI to adapt the interleaver structure to the channel response. We propose to exploit CSI at the transmitter to design an adaptive interleaver for a specific convolutional code, channel response and constellation in Bit-Interleaved Coded Modulation (BICM) for OFDM systems.

Traditionally, the goal of the bit interleaver in BICM is to break the temporal structure of the channel providing a diversity gain in systems with no CSI at the transmitter, which reduces the bit error rate (BER) at the decoder output [2]. Alternatively, when CSI is available at the transmitter this information can be exploited to design an interleaver matched to the channel response, which strategically reallocates the bits to be transmitted according to their relevance on the error correction capability of the code. In [3] Sai-Weng Lei et al. proposed an adaptive interleaver for OFDM systems based on

Paper approved by I. Lee, the Editor for Wireless Communication Theory of the IEEE Communications Society. Manuscript received October 15, 2007; revised June 28, 2008 and September 17, 2008.

The authors are with the Department of Signal Theory and Communications, Technical University of Catalonia (UPC), c/ Jordi Girona 1-3, Mòdul D5, Campus Nord UPC, 08034 Barcelona, Spain (e-mail: {francesc.rey, gregori.vazquez}@upc.edu; xell@gps.tsc.upc.edu).

This work was supported in part by the Spanish Government under Grant TEC2007-68094-C02-2, and CONSOLIDER CSD2008-00010, and the Catalan Government (DURSI) under Grant 2005SGR-00639.

Digital Object Identifier 10.1109/TCOMM.2009.06.070141

a regular distribution of the transmitted symbols as a function of the channel state, ensuring that two consecutive symbols were never subject to similar channel gains. This adaptive interleaver exploited the knowledge of the instantaneous fading but did not take into account the structure of the convolutional code, of great importance for the coded BER performance.

This letter proposes an adaptive bit interleaver that, unlike the symbol interleaver proposed in [3], it takes into account the specific convolutional code and the constellation employed in the BICM-OFDM scheme. Such interleaver, named '*RCPC-based interleaver*', is based on Rate-Compatible Punctured Convolutional Codes (RCPC codes) [4] and uses the puncturing tables of this family of codes to decide how bits are mapped to the symbols and allocated to the subcarriers. The metric employed to design the adaptive interleaver is the mutual information between the encoded bits and the corresponding log-likelihood ratios (LLR) at the BICM demodulator output [2].

The procedure to design the proposed interleaver is illustrated by its application to the air interface of the IEEE802.11a standard [5]. The simulation results for this example indicate that the proposed adaptive interleaver provides significant performance gains in terms of packet error rate (PER) at the expense of a small complexity increase. The numerical results also evidence the importance of the specific interleaver when comparing the performance of different power allocation strategies in convolutionally coded systems.

II. SYSTEM MODEL

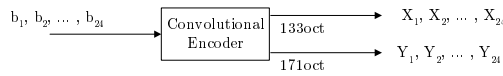
This section describes the BICM-OFDM system in which the proposed adaptive interleaver is used. The information bit stream to be transmitted is first encoded with a convolutional code. Next, the bits are interleaved, mapped into constellation symbols, and finally modulated into OFDM symbols. Optionally a power allocation strategy can be used to distribute the power among the subcarriers before the OFDM modulation stage.

Let us assume that the channel keeps invariant during the transmission of one codeword and the length of the OFDM cyclic prefix has been appropriately chosen according to the channel impulse response length. Then, denoting K the number of subcarriers per OFDM symbol, the signal r_k received at the k th subcarrier for each OFDM symbol can be written as:

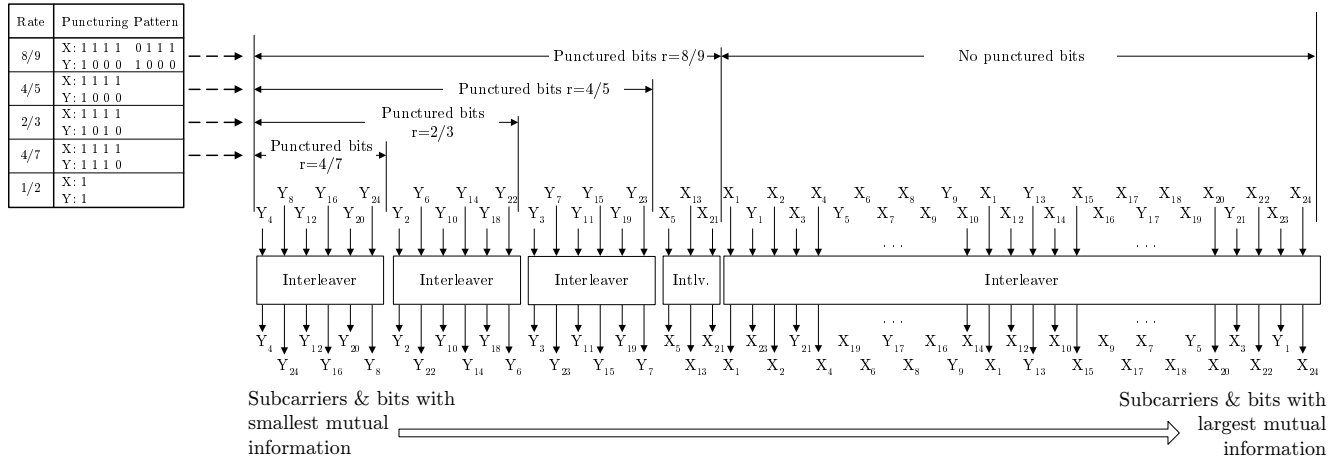
$$\begin{aligned} r_k &= \gamma_k \sqrt{P_k} s_k + n_k \\ &= H_k s_k + n_k \quad k = 0, \dots, K-1 \end{aligned} \quad (1)$$

where s_k is the unit variance constellation symbol transmitted in the k th subcarrier (assuming that b bits are transmitted per

Encoder:



Interleaver:

Fig. 1. RCPC based interleaver pattern. Example for IEEE802.11a. $K=48$, $N=2$, $P=8$, $b=1$ (BPSK constellation).

symbol), H_k collects the channel gain γ_k and power allocation P_k (when this stage is considered at the transmitter), and n_k is the additive white Gaussian noise term with zero mean and variance σ_n^2 .

At the receiver, the demapper computes the bit LLR's from the symbols at the channel output following a classical BICM demapper (see equation (7) in [2]). These LLR's are next deinterleaved and finally used to detect the information sequence applying a maximum likelihood decoder based on the Viterbi algorithm. Taking into account the system model in (1) with K subcarriers and b bits per symbol, this BICM-OFDM operation yields a set of $K \cdot b$ parallel independent and memoryless binary subchannels. Each subchannel has a different quality measured as the mutual information between the i th bit of the transmitted symbol at the k th subcarrier and the corresponding LLR at the BICM demodulator output (see equation (12) in [2]).

The design of the adaptive interleaver requires CSI at the transmitter, which can be provided through a feedback channel. The techniques to design the feedback link are out of the scope of this letter. Several references are available in the literature dealing with this important point (e.g., see [6], [7]). Specifically, in [7] it is concluded that only 2 bits per channel coefficient are enough to track the channel when two identical channel predictors are used at both sides of the link. Note that if the CSI at the transmitter is employed only for the design of the interleaver, then this quantity could be further reduced because full CSI would not be required, as evidenced in the following paragraphs.

A. Upper bound on the word error probability

Denoting \mathbf{c}_0 the transmitted sequence that maps the sequence of coded bits into constellation symbols, and denoting the channel matrix \mathbf{H}_{Π} the diagonal matrix whose entries are the K fading coefficients deinterleaved and repeated as many times as OFDM symbols needed to transmit \mathbf{c}_0 , the squared

Euclidean distance between two noiseless coded sequences at the channel output, hereafter named as received codewords, is defined as: $D(\mathbf{c}_0, \mathbf{c}_i | \mathbf{H}_{\Pi}) = \|\mathbf{H}_{\Pi}(\mathbf{c}_0 - \mathbf{c}_i)\|^2$. Then, for any channel code with maximum likelihood decoding, the word error probability conditioned to a realization of the channel propagation \mathbf{H}_{Π} can be upper-bounded using the union bound as follows [8]:

$$\begin{aligned}
 P(e | \mathbf{H}_{\Pi}) &\leq \sum_{\mathbf{c}_i \neq \mathbf{c}_0} P(\mathbf{c}_0 \rightarrow \mathbf{c}_i | \mathbf{H}_{\Pi}) \\
 &= \sum_{\mathbf{c}_i \neq \mathbf{c}_0} Q\left(\sqrt{\frac{D(\mathbf{c}_0, \mathbf{c}_i | \mathbf{H}_{\Pi})}{2N_o}}\right) \quad (2)
 \end{aligned}$$

where $P(\mathbf{c}_0 \rightarrow \mathbf{c}_i | \mathbf{H}_{\Pi})$ is the conditional pairwise error probability (PEP) of detecting the transmitted sequence \mathbf{c}_i when \mathbf{c}_0 was transmitted given a specific channel realization, $N_o/2$ is the noise variance per real component and $Q(\cdot)$ is the Gaussian Q-function.

As shown in (2) the error probability is directly related with the Euclidean distance $D(\mathbf{c}_0, \mathbf{c}_i | \mathbf{H}_{\Pi})$, whose dependence with the interleaver appears on the channel matrix \mathbf{H}_{Π} : for a given $(\mathbf{c}_0, \mathbf{c}_i)$ pair and a specific channel realization the specific interleaver determines the ordering of the channel coefficients in \mathbf{H}_{Π} . In Section IV-A this Euclidean distance will be used to illustrate the gain of the proposed adaptive interleaver.

III. RCPC-BASED INTERLEAVER

The adaptive interleaver proposed in this letter is based on Rate-Compatible Punctured Convolutional Codes. The RCPC codes are a family of variable-rate convolutional codes introduced in [4] extending the concept of punctured convolutional codes. These codes are constructed by puncturing a low rate convolutional code $R = 1/N$ (named mother code) to obtain a family of codes with rate $P/(P+l)$, where P is the puncturing period and l can be varied between 1 and $(N-1)P$.

The puncturing procedure follows a rate-compatible criterion, which ensures that all code bits of a high rate punctured code are used by all the lower rate codes (i.e., the high rate codes are embedded into the lower rate codes of the family). Hence, the transmitted signal can be encoded at different rates without increasing the decoder complexity. Tables in [4], [9], [10] report the puncturing patterns for RCPC codes that provide the maximum free distance.

The RCPC-based interleaver proposed in this letter does not introduce any puncturing in the encoded bits but it uses the puncturing tables to map the bits to the symbols and to allocate them to the different subcarriers. The metric to design the adaptive interleaver is the mutual information between the i th bit of the transmitted symbol at the k th subcarrier and the corresponding LLR at the BICM demapper output. Following the principle that the bits with the lowest mutual information will be the least reliable bits at the receiver, the interleaver assigns the coded bits in the same order as they would be punctured in a RCPC code. Thus, the bits that are first punctured in this family of codes are mapped to positions with the lowest mutual information, whereas the bits that are never punctured are located to the largest mutual information positions. Note that the design of this adaptive interleaver does not require to know the channel response at the transmitter but only the ranking of the mutual information for each subchannel in a smallest-to-largest sorting¹.

Next, we illustrate the procedure for designing the adaptive interleaver. We describe the interleaver scheme for the convolutional code of rate $1/N$ ($N = 2$) with generator polynomials 133_{OCT} and 171_{OCT} (used in different communication standards like IEEE802.11a, IEEE802.16 or DVB-T and DVB-S) using the puncturing pattern derived in [4] with period $P = 8$ (this puncturing pattern is shown in Figure 1). The extension to other convolutional codes is straightforward by simply using the appropriate puncturing pattern. The interleaver is described for an arbitrary number of subcarriers K and any constellation with b bits per symbol, although for the sake of simplicity Figure 1 displays the adaptive interleaver pattern for $K = 48$ subcarriers and $b = 1$ (BPSK constellation).

First, we collect the encoded bits into groups of $K \cdot b$ consecutive bits. Next, the puncturing pattern with period P , chosen for the mother code of rate $1/N$, is extended $T = \frac{K \cdot b}{N \cdot P}$ times to obtain a puncturing pattern for the $K \cdot b$ encoded bits. Note that the period P must be chosen to satisfy T to be an integer, otherwise an adaptive interleaver that varies from OFDM symbol to OFDM symbol would be designed. Then, the encoded bits are grouped following the extended puncturing pattern. In the example of Figure 1 the first group of bits is composed by the encoded bits that should be removed to obtain the punctured code of rate $4/7$, which correspond to the bits $Y_4, Y_8, Y_{12}, Y_{16}, Y_{20}, Y_{24}$ in a sequence of 48 encoded bits. The second group is composed by the bits that should be punctured to obtain the code of rate $2/3$. This procedure is repeated to get the third and fourth groups with the bits that were punctured for the rates $4/5$, and

$8/9$, respectively. Finally, the remaining bits, which are never punctured, constitute the last group of encoded bits. As the puncturing pattern only provides a finite set of rates we are not able to define any priority in the bits that belong to the same group. Hence, for each group an interleaver that reorders the position of the different bits inside the group is introduced. In the paper we propose an interleaver that reverses the order of the even bits to guarantee that two consecutive bits in a group are not allocated in the same deepest or strongest subcarrier of that group (see Figure 1). This interleaver becomes of particular interest when we have a large number of encoded bits $K \cdot b$ (notice that the optimal way to assign the carriers to those bits would require the design of a puncturing pattern with $P = K \cdot b/N$, however, we discard this choice since the complexity of this task might not be affordable for large values of $K \cdot b$). Finally, the resulting sequence of interleaved bits are mapped to the symbols and allocated to the subcarriers in ascending order of the mutual information.

IV. PERFORMANCE EVALUATION

The performance of the proposed adaptive interleaver is compared in this section with two additional interleavers: the block interleaver defined in the IEEE 802.11a standard [5] (named '*Block standard interleaver*') and the adaptive symbol interleaver described in [3] (named '*Adaptive symbol interleaver*'). The comparison is done in terms of the squared Euclidean distances between two received codewords (Section IV-A), and also in terms of the packet error rate (PER) (Section IV-B). The robustness of the algorithm with respect to CSI uncertainty is shown in Section IV-C. Finally, different power allocation strategies are evaluated in Section IV-D in order to analyze the interplay between the interleaver and the power allocation policy.

The simulation parameters have been selected according to the IEEE 802.11a standard [5]. The convolutional code of rate $1/2$ is initialized to the zero state and returned to it after each packet, whose length is set to $M = 1728$ coded bits (i.e. 18 OFDM symbols). Those bits are interleaved and mapped into QPSK or 16QAM constellation symbols with Gray mapping. The channel follows a multipath Rayleigh fading channel with an impulse response that obeys an exponential power delay profile with delay spread 150ns ($PDP(\tau) = e^{-\tau/150ns}$ [11]). This channel, based on the BRAN C channel model, models a typical open space environment with non-line-of-sight conditions [12]. The channel has been implemented with a 16-tap delay line [11], which is close to the maximum channel length permitted by the cyclic prefix, with taps equispaced 50ns.

A. Evaluation of the Euclidean distance between two received codewords

In this section the influence of the interleaver on the error probability is analyzed. We evaluate the cumulative density function of the squared Euclidean distances between the received codewords for QPSK modulation with Gray labeling (see Section II-A).

This evaluation requires exhaustive listing of all the codewords. Thanks to the uniform error property of linear convolutional codes and the use of QPSK modulation with Gray labeling, this evaluation can be simplified assuming that the all-zero

¹Although the mutual information is proposed in the paper (and used in the numerical results) as a metric to rank the subcarriers, a more simple, but suboptimal, design could be implemented ranking the subcarriers according to the channel gains.

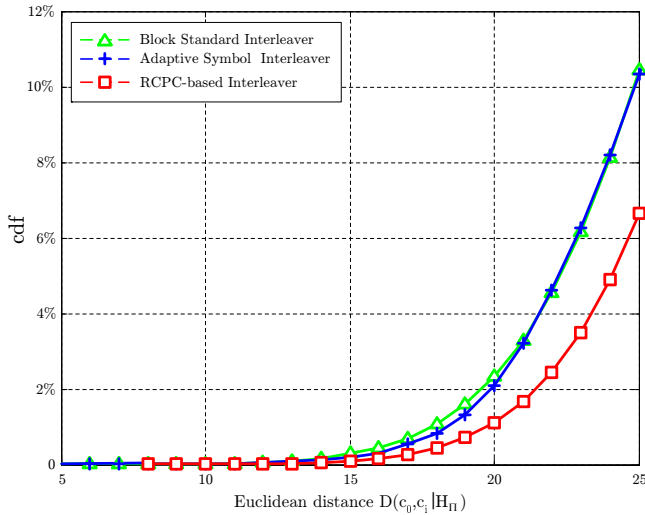


Fig. 2. Cumulative density function of the squared Euclidean distance for different interleavers.

sequence was transmitted. Moreover, we focus the attention on the codewords with small Euclidean distance because the error probability strongly depends on those terms at high SNR. Assuming that the codewords with small Hamming weight are related with the smallest Euclidean distances, we have considered only those terms to calculate the cumulative density function. A large amount of convolutional code sequences was generated requiring intensive computation. We stopped the computation after obtaining all coded sequences of length 1728 coded bits with Hamming weight $w_d \leq 16$, 90% of all coded sequences of length 1728 coded bits with Hamming weight $w_d = 18$ and 22% of all coded sequences of length 1728 coded bits with Hamming weight $w_d = 20$.

Figure 2 illustrates the cumulative density function of the squared Euclidean distance for the different interleavers focusing the attention on the smallest distances. The results are presented for a specific channel realization and uniform power allocation, although similar results were obtained for other channel realizations or power allocation policies. Note that the RCPC-based interleaver provides larger Euclidean distances when compared with the other two interleavers. This significant improvement in the spectrum of distances results in a better performance in terms of PER as shown in the next section. Moreover, it can be shown that the RCPC-based interleaver provides the largest minimum Euclidean distance. Specifically, in this particular channel realization the minimum Euclidean distance when the RCPC-based interleaver is employed is $D_{min} = 8.61$ whereas the distance reduces to $D_{min} = 5.31$ and $D_{min} = 5.75$ for the *Adaptive symbol interleaver* and the *Block standard interleaver*, respectively.

B. Packet Error Rate

This section evaluates the performance of the interleavers in terms of PER. Figure 3 compares the PER performance for the different interleavers when a uniform power allocation (solid lines) and a power allocation policy that maximizes the channel capacity [13] (dotted lines) are considered. We present the results for QPSK and 16QAM constellations. The

conclusions are coherent with those drawn in the previous section: the RCPC-based interleaver outperforms the other two interleavers. For QPSK constellation and uniform power allocation the E_b/N_0 improvement of the RCPC-based interleaver at $PER = 10^{-2}$ is 0.6dB when compared with the adaptive interleaver proposed in [3] and 1.0dB when compared with the block interleaver defined in the IEEE 802.11a standard [5]. Similarly, the E_b/N_0 gains when the power is allocated to maximize the channel capacity are 0.9dB and 1.4dB, respectively. For 16QAM constellation the RCPC-based interleaver offers similar gains. Specifically, the gain is 0.6dB and 0.9dB for uniform power allocation and 0.8dB and 1.3dB for the maximum capacity power allocation.

Comparing the performance when the power is allocated uniformly to the performance when the power is allocated to maximize the channel capacity, it is somewhat surprising that only the RCPC-based interleaver presents a gain in the second case. This result evidences the dependency of power allocation performance on the interleaver choice, and it is analyzed in Section IV-D.

C. Performance vs. CSI quality at the transmitter

Next, we present some numerical experiments to test the sensitivity of the proposed adaptive interleaver against channel uncertainty. This channel uncertainty is modeled as an additive term to the channel impulse response, assumed to be a zero mean Gaussian process independent of the true channel [7]. Figure 4 shows the minimum E_b/N_0 required to achieve a $PER \leq 10^{-2}$ for QPSK and 16QAM and uniform power allocation as a function of the channel uncertainty degree at the transmitter, measured by the coefficient ρ :

$$\rho = \frac{\sigma_\epsilon^2}{\sigma_\epsilon^2 + \sigma_h^2} \quad (3)$$

where σ_h^2 is the power of the channel, σ_ϵ^2 is the variance of the channel error. Hence, $\rho = 0$ denotes perfect CSI and $\rho = 1$ means no channel knowledge.

As shown, the performance of the RCPC-based interleaver slightly degrades when only partial CSI is available. Moreover, the performance of the proposed interleaver tends to the performance of the *Block standard interleaver* when no channel information is available. These results evidence the robustness of the RCPC-based interleaver to imperfect CSI.

D. Comparison for different power allocation strategies

Table I shows the E_b/N_0 required to achieve a $PER=10^{-2}$ for different power allocation strategies and QPSK constellation. The algorithms are labeled as follows: '*Capacity*' refers to the power allocation strategy that maximizes the channel capacity [13]; '*R₀*' denotes the algorithm that maximizes the cut-off rate [14]; '*Unc. BER*' refers to the algorithm that minimizes the uncoded BER [15]; '*MMSE*' designates the algorithm that maximizes the Mean-Squared Error [16]; '*Uniform*' indicates that the same power is allocated to all the subcarriers. For a better understanding of those results it is worth to mention that when the power is non-uniformly allocated the transmitted symbols observe an equivalent channel H_k whose statistics depend on the power allocation criterion and are different

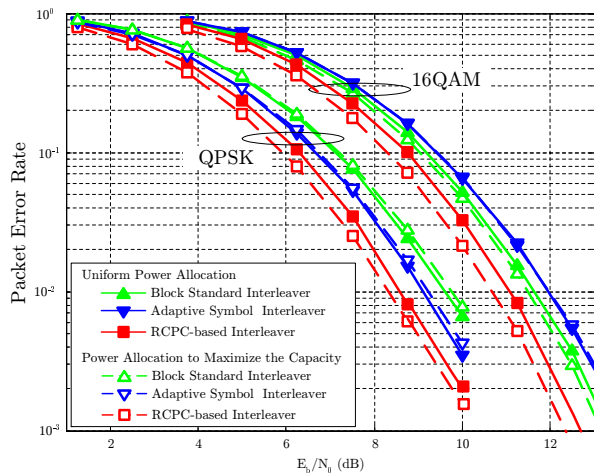


Fig. 3. PER comparison for different interleavers. Power allocation strategy: uniform (solid lines) and max. capacity (dotted lines).

TABLE I
 E_b/N_0 (dB) required to achieve a $PER = 10^{-2}$ (QPSK
CONSTITUTION).

Power Allocation	Interleaver		
	RCPC-based	Adaptive Symbol [3]	Block Standard [5]
Capacity	8.3	9.2	9.7
R_0	7.8	8.5	8.9
Unc. BER	8.0	8.3	9.0
MMSE	8.2	8.5	9.0
Uniform	8.6	9.2	9.6

from the statistics of the channel gain γ_k (typically a Rayleigh fading channel). Some algorithms (e.g., 'Capacity' and ' R_0 ') tend to allocate scarce or null power to the worst subcarriers, redistributing this power among the remaining subcarriers [7]. On the contrary, other algorithms like the 'Unc. BER' tend to the zero-forcing solution, causing a flat channel response [7]. The differences in the power allocation policies can be used to analyze in Table I the performance of the different interleavers. First, it is important to note that the RCPC-based interleaver always outperforms the rest of interleavers independently of the specific power allocation strategy. Note also that the power allocation strategies with a larger gain in terms of E_b/N_0 are those with a large number of null subcarriers (i.e., the 'Capacity' and ' R_0 '), whereas the gain is reduced for the algorithms that null less subcarriers (e.g., the 'Unc. BER' algorithm). This result can be explained noting that when there is a large number of null/damaged subcarriers, only the RCPC-based interleaver rightly decides which are the bits to be allocated in those subcarriers, distributing the coded bits in the same order as they would be punctured in a RCPC code.

Results in Table I are also important to evidence the importance of the interleaver when comparing the performance of different power allocation strategies. Note, for example, that the algorithm that minimizes the uncoded BER could be concluded to be the best algorithm in terms of PER if the interleaver in [3] were used, whereas it is not the best one with other interleavers.

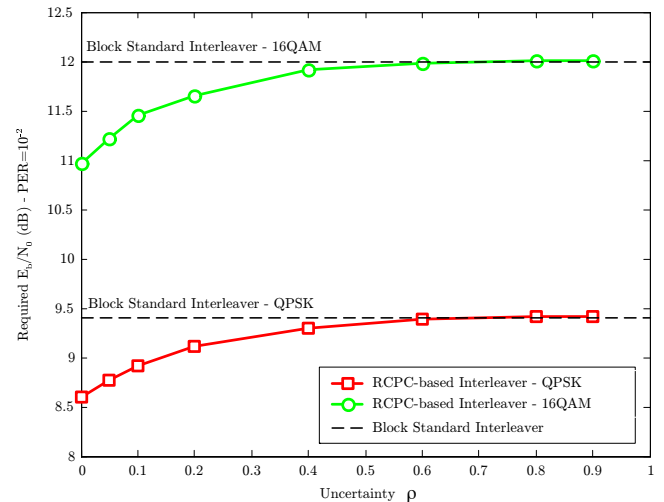


Fig. 4. Minimum E_b/N_0 that achieves a $PER \leq 10^{-2}$ vs transmitter uncertainty ρ .

V. CONCLUSIONS

This letter has presented the design of an adaptive interleaver based on RCPC codes making use of the CSI at the transmitter. Specifically, this interleaver rearranges the bits as a function of the mutual information between the transmitted bits and the corresponding log-likelihood ratios at the demapper output using the rate-compatible puncturing patterns employed to design the family of RCPC codes. Contrary to other adaptive interleavers, the RCPC-based interleaver is designed for a specific convolutional code and constellation, and thus distributes the bits more effectively.

The RCPC-based interleaver outperforms other interleavers in the literature in terms of packet error rate thanks to an increase in the Euclidean distances between the received codewords. As shown, the gain of the proposed interleaver increases as the number of deep-faded subcarriers increase or when some power allocation strategy similar to waterfilling is used. Numerical results have also shown the importance of the interleaver when comparing the performance of different power allocation strategies with convolutional codes.

REFERENCES

- [1] J. Campello, "Practical bit loading for DMT," in *Proc. Int. Conf. Communications (ICC99)*, pp. 801-805, Vancouver, Canada, June 1999.
- [2] G. Caire, G. Taricco, and E. Biglieri, "Bit-interleaved coded modulation," *IEEE Trans. Inform. Theory*, vol. 44, no. 3, pp. 927-946, May 1998.
- [3] S.-W. Lei and V. K. N. Lau, "Performance analysis of adaptive interleaving for OFDM systems," *IEEE Trans. Veh. Technol.*, vol. 51, no. 3, pp. 435-444, May 2002.
- [4] J. Hagenauer, "Rate-compatible punctured convolutional codes (RCPC Codes) and their applications," *IEEE Trans. Commun.*, vol. 36, no. 4, pp. 389-400, Apr. 1988.
- [5] IEEE802.11, "IEEE Std 802.11a-1999, Supplement to IEEE Standard for Information Technology, Part 11: Wireless LAN Medium Access Control(MAC) and Physical Layer (PHY) specifications: High-Speed Physical Layer in the 5 GHz Band," Institute of Electrical and Electronics Engineers, 1999.
- [6] G. Jöngren and M. Skoglund, "Quantized feedback information in orthogonal spacetime block coding," *IEEE Trans. Inform. Theory*, vol. 50, no. 10, pp. 2473-2482, May 2004.
- [7] F. Rey, "Feedback-channel and adaptive MIMO coded-modulations," Ph.D. thesis, UPC, Nov. 2005.

- [8] J. G. Proakis and M. Salehi, *Communication Systems Engineering*. Prentice Hall Int. Ed., 1994.
- [9] L. H. C. Lee, "New rate-compatible punctured convolutional codes for Viterbi decoding," *IEEE Trans. Commun.*, vol. 42, no. 12, pp. 3073–3079, Dec. 1994.
- [10] P. K. Frenger, P. Orten, T. Ottosson, and A. B. Svensson, "Rate-compatible convolutional codes for multirate DS-CDMA systems," *IEEE Trans. Commun.*, vol. 47, no. 6, pp. 828–836, June 1999.
- [11] T. S. Rappaport, *Wireless Communications: Principles and Practice*. Englewood Cliffs, NJ: Prentice Hall, 1996.
- [12] J. Medbo, P. Schramm, "Channel models for HIPERLAN/2 in different indoor scenarios," ETSI BRAN 3ERI085B, Mar. 1998.
- [13] T. Cover and J. A. Thomas, *Elements of Information Theory*. John Wiley & Sons, 1991.
- [14] F. Rey, M. Lamarca, and G. Vazquez, "A transmitter design for coded systems in the presence of CSI errors," in *Proc. 37th Asilomar Conf. Signals, Syst. Comput.*, pp. 1065–1069, Pacific Grove, CA, USA, Nov. 2003.
- [15] F. Rey, M. Lamarca, and G. Vazquez, "Robust power allocation algorithms for MIMO OFDM systems with imperfect CSI," *IEEE Trans. Signal Processing*, vol. 53, no. 3, pp. 1070–1085, Mar. 2005.
- [16] S. Barbarossa and A. Scaglione, "Time-varying channels," in *Signal Processing Advances in Wireless Communications*, G. B. Giannakis, Y. Hua, P. Stoica, and L. Tong, eds., vol. II: Trends in Single- and Multi-User Systems, chapter 1. Prentice-Hall, 2000.